Available online at www.sciencedirect.com
SCIENCE DIRECT®
Catalysis Today 87 (2003) 3–10
CATALYSIS TODAY
www.elsevier.com/locate/cattod

Decomposition of NH_3 over Zn–Ti-based desulfurization sorbent promoted with cobalt and nickel

Hee Kwon Jun [a], Suk Yong Jung [a], Tae Jin Lee [b], Chung Kul Ryu [c], Jae Chang Kim [a,*]

[a] *Department of Chemical Engineering, Kyungpook National University, Daegu 702-701, South Korea*
[b] *School of Chemical Engineering and Technology, Yeungnam University, Kyongsan 712-749, South Korea*
[c] *Korea Electric Power Research Institute, Daejon 305-380, South Korea*

Abstract

Zn–Ti-based sorbents promoted with cobalt and nickel additive were prepared by simple physical mixing of single oxides. Their capacities for removing H_2S and NH_3 simultaneously, emitted from coal gasifiers, were investigated in a micro-reactor at 1 atm and 650 °C. NH_3 within the fuel gases did not affect the sulfur removing capacity of the Zn–Ti-based sorbent. The additives, cobalt and nickel, were found to be active components in NH_3 decomposition as well as H_2S absorption, while major components such as ZnO and TiO_2 did not show any activity in the NH_3 decomposition reaction. NH_3 was decomposed over both oxide and sulfide forms of the additives, even though the NH_3 decomposition ability of their sulfides dramatically decreased in the presence of H_2 gas owing to the equilibrium limitation of NH_3 decomposition. In the case of oxide forms, cobalt oxide showed excellent NH_3 decomposition capacity regardless of H_2 concentrations, while the capacity of nickel oxide depended on the H_2 concentrations.

Keywords: Desulfurization; NH_3 decomposition; Zn–Ti based sorbent

1. Introduction

The integrated gasification combined cycle (IGCC) is considered to be one of the most efficient and environmentally acceptable technologies for generating power from coal. To use this technology, it is necessary to remove the pollutants from the coal-derived fuel gas. Among the pollutants, sulfur and nitrogen, which exist in the form of hydrogen sulfide (H_2S) and ammonia (NH_3) under the highly reducing conditions of a gasifier, must be removed from the hot coal gas because both species entering the gas turbine are converted to SO_x and NO_x, which are known precursors of acid rain and whose emission into the atmosphere is limited by strict government regulations. To remove hydrogen sulfide and ammonia from coal-derived gas, several metal oxide materials have been studied to develop regenerable sorbents in high- and middle-temperature ranges under the highly reducing conditions of a gasifier [1–25]. However, the roles of additives and supporters have not been clearly defined in these operating conditions because of the lack of identification of new active sites and their mechanisms. In particular, the research for simultaneously removing H_2S and NH_3 on regenerable sorbents requires more effort. The major objectives of this work were to identify any deleterious changes in the ZT-based sorbents caused by NH_3 in a fixed-bed reactor, the role of additives such as cobalt and nickel in the presence of NH_3, and the reaction mechanism for

* Corresponding author. Tel.: +82-53-950-5622; fax: +82-53-950-6615.
E-mail address: kjchang@knu.ac.kr (J.C. Kim).

0920-5861/$ – see front matter © 2003 Elsevier B.V. All rights reserved.
doi:10.1016/j.cattod.2003.10.013

the simultaneous removal reaction of H_2S and NH_3 under strong reducing condition at high temperature.

2. Materials and methods

2.1. Preparation of the sorbent

Zinc titanate (ZT) and modified (ZTC, ZTN) sorbents used in this study were prepared by physical mixing. Zinc oxide, titanium dioxide, and cobalt or nickel oxide, of which the particle size was about 200–300 mesh, were sufficiently mixed with an inorganic binder, bentonite, for 1–2 h. Next, a liquid binder, ethylene glycol (EG), was added to the mixture in order to make a slurry. An extruder was used to form pellets with an outer diameter of 1 mm from the slurry. These wet pellets were dried for 4 h to remove EG from the material in a temperature range 250–300 °C. The dried pellets were calcined in a muffle furnace for 12 h at 700 °C, and then ground to particle size in a range 250–300 μm in diameter. The ramping rate of the temperature was maintained at 3 °C/min. The mole ratio of Zn to Ti and the amounts of additives added were fixed at 1.5:1 and 20 wt.%, respectively. In addition, X-ray diffraction (XRD) was performed to identify crystalline phases in the mixed oxides. A Philips XPERT instrument using Cu Kα radiation was used to do so.

2.2. Apparatus and procedure

Multiple cycles of sulfidation/regeneration were performed in a fixed-bed quartz reactor with a diameter of 1 cm placed in an electric furnace. One gram of sorbent was packed into the reactor and the space velocity (SV) was maintained at 5000 h^{-1} to minimize severe pressure drops and channeling phenomena. All the volumetric flows of gas were measured at standard temperature and pressure (STP) conditions. The temperature of the inlet and outlet lines of the reactor was maintained above 120 °C to prevent condensation of water vapor in the sulfidation processes. The outlet gases from the reactor were automatically analyzed every 8 min by a thermal conductivity detector (TCD) equipped with an autosampler (Valco). The column used in the analysis was a 1/8 in. Teflon tube packed with Porapak T. The conditions of sulfidation and regeneration and the composition of mixed gases are shown in Table 1. When the H_2S concentration of the outlet gases reached 10,000 ppm, the concentration of H_2S at the inlet stream of mixed gases, an inert nitrogen gas without H_2S, was introduced to purge the system until it reached the regeneration temperature. Finally, nitrogen gas mixed with 3% oxygen was introduced to regenerate the sulfurized sorbents until the SO_2 concentration reached 200 ppm.

Table 1
Experimental conditions for Zn–Ti-based sorbents

	Sulfidation	Regeneration
Temperature (°C)	650	800
Pressure (atm)	1	5
Flow rate (ml/min)	50	50
Gas composition (vol.%)		
H_2S	1.0	
H_2	11.7	
CO	9.6	
CO_2	5.2	
N_2	Balance	Balance
O_2		3–5

3. Results and discussion

3.1. Structure identification

Fig. 1 shows the XRD results of various sorbents before/after H_2S absorption at 650 °C. ZT sorbent before H_2S absorption consists of a separated ZnO and TiO_2 phase without the spinel structure like Zn_2TiO_4 owing to the low calcination temperature. After H_2S absorption, most of the separated ZnO was transformed to ZnS and no unreacted ZnO was observed. It was also found that TiO_2 did not participate in H_2S absorption. The XRD pattern of ZTN before H_2S absorption showed a separated ZnO, TiO_2, and NiO phase, but only ZnS and TiO_2 were observed without nickel sulfides after H_2S absorption. It has already been reported that the nickel sulfide formed after H_2S absorption was amorphous phases [8]. In the case of ZTC sorbent, Co_3O_4 peaks were observed together with the spinel structure in the XRD pattern before H_2S absorption. After H_2S absorption, it was found that most of the metal oxides were transformed to the ZnS/Co_9S_8 without unreacted oxides phases.

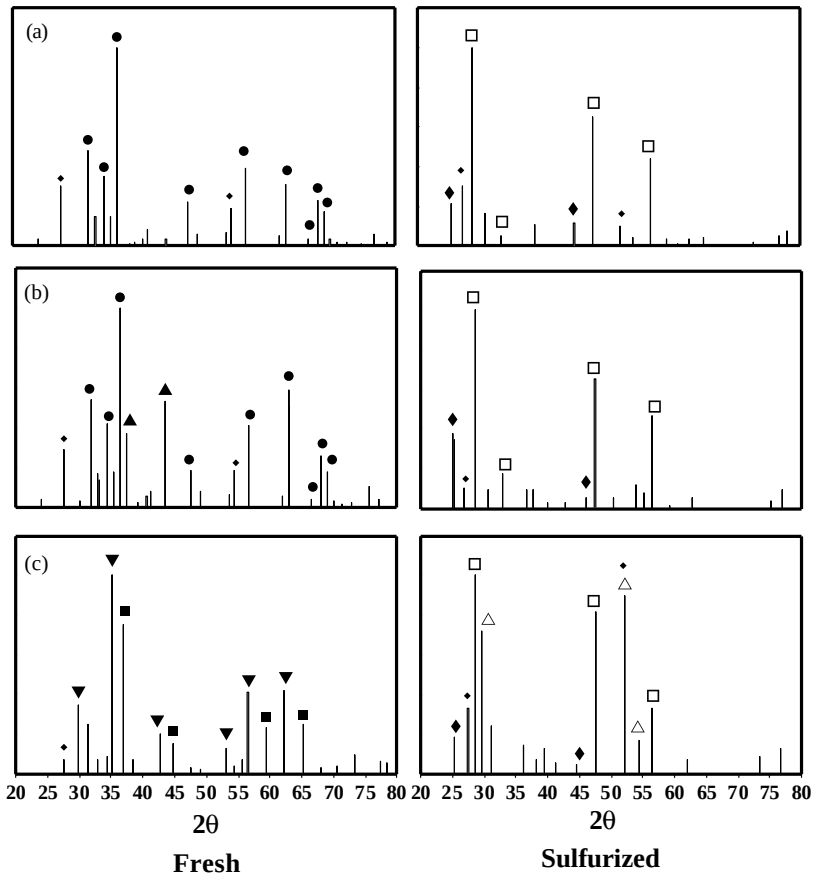

Fig. 1. XRD patterns of various sorbents before/after sulfidation at 650 °C: (a) ZT; (b) ZTC; (c) ZTN; (●) ZnO; (▼) Zn_2TiO_4; (⧫) TiO_2 (rutile); (◆) TiO_2 (anatase); (■) Co_3O_4; (▲) NiO; (□) ZnS; (△) Co_9S_8.

3.2. H_2S performance and NH_3 removal

Fig. 2 shows the H_2S breakthrough curves of various Zn–Ti-based sorbents in gas compositions with 5000 ppm of NH_3 and 1% of H_2S at 650 °C. The *X*-axis and *Y*-axis indicate reaction time and H_2S concentration emitted from the reactor, respectively. The total sulfur removal capacity calculated from this graph was higher than 25 wt.%, which was similar to the value previously reported [8]. This result indicates that the NH_3 included in the mixed gas does not affect the total sulfur removal capacity of the sorbents under our experimental conditions. Fig. 3 shows NH_3 removing capacity of various sorbents with a reaction time at 650 °C. The ZT sorbent without any promoter showed very low NH_3 decomposition re-

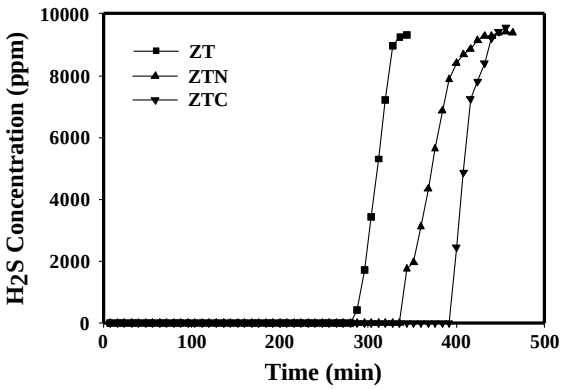

Fig. 2. H_2S breakthrough curves of various sorbents at 650 °C.

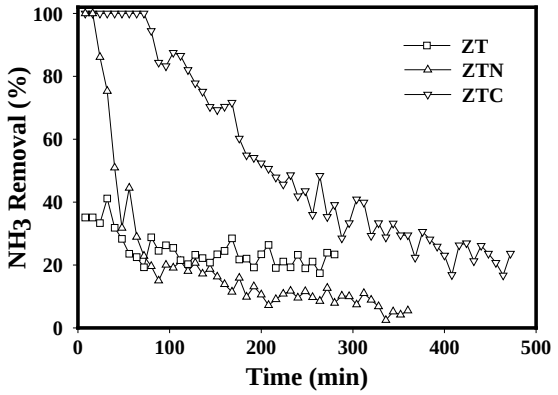

Fig. 3. Decomposition of NH_3 on various sorbents at 650 °C.

activity (20–30% even at initial period). However, in the case of the ZTC and ZTN sorbent, promoted with cobalt and nickel, respectively, 100% of NH_3 decomposition was observed in the initial period and the reactivity gradually decreased with reaction time. In coal-derived gases, the decomposition of NH_3 on these Zn–Ti-based sorbents was not easy because the initial metal oxides were transformed to metal sulfides during the H_2S absorption and H_2 gas prevented the NH_3 decomposition due to the equilibrium limitation.

3.3. Thermal decomposition of NH_3 and the effect of product gas

Fig. 4 shows NH_3 decomposition in the empty reactor as a function of reactor temperature. NH_3 decomposition was not observed until 550 °C and above 600 °C, gradually increased with temperature. 80% of the NH_3 was decomposed at 800 °C. Considering that most experiments were carried out at 650 °C, about 40% of the NH_3 was removed by thermal decomposition. Because the decomposition of NH_3 generates N_2 and H_2, the presence of H_2 in the reactant mixture was believed to prevent NH_3 gas from decomposing. Thermal decomposition of NH_3 was investigated with various H_2 concentrations in an empty reactor at 650 °C. As shown in Fig. 5, thermal decomposition of NH_3 decreased with increasing H_2 concentration and was not observed at H_2 concentrations higher than 20%. Considering that 10% of H_2 was contained in our mixed gas, 10% of the NH_3 was decomposed only by thermal reaction. Fig. 6 shows the NH_3 decomposition of various sorbents before H_2S absorption with various H_2 concentrations. The NH_3 decomposition of ZT sorbent showed 0–40% with H_2 concentrations, which was similar to the results observed in the empty reactor. At that time, H_2S was not included with gas compositions. Considering that the ZT sorbent has a separated ZnO and TiO_2 phase as shown in Fig. 1(a), it was found that both ZnO and TiO_2 did not participate in NH_3 decomposition at this experimental condition. NH_3 decomposition of the ZTN sorbent showed 100% without H_2, but the reactivity gradually decreased with increased H_2 concentration. In the case of ZTC sorbent, 100% NH_3 was decomposed in an H_2 concentration less than 10%, gradually decreasing with reaction time at H_2 concentrations higher than 20%.

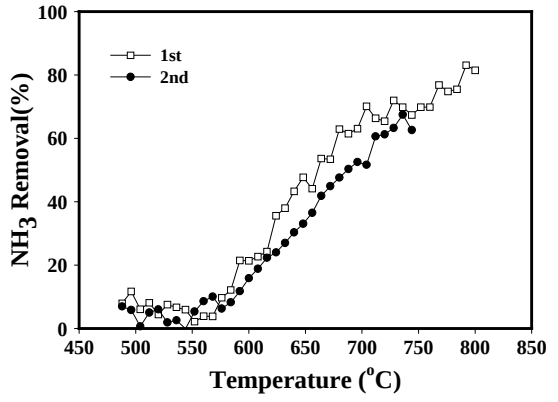

Fig. 4. Thermal decomposition of NH_3 with increasing temperatures in empty reactor.

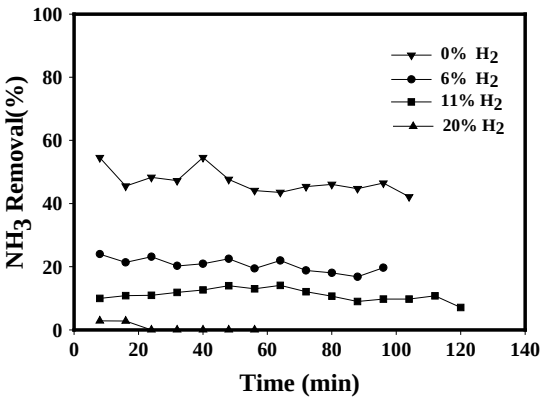

Fig. 5. Thermal decomposition of NH_3 with various H_2 concentrations in empty reactor.

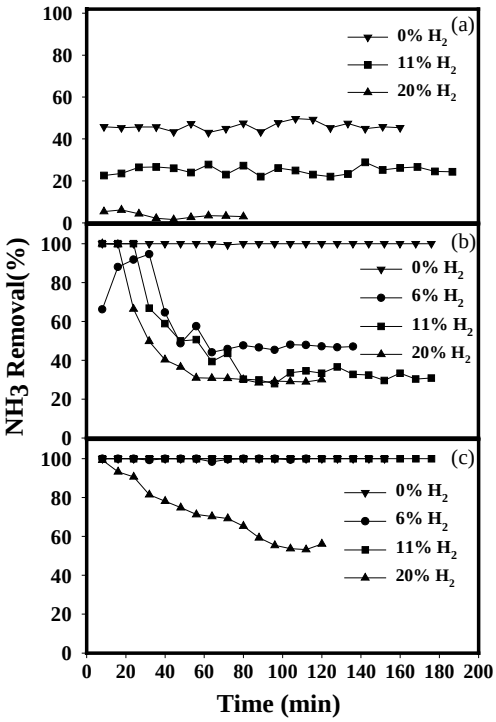

Fig. 6. NH_3 decomposition of various sorbents with various H_2 concentrations: (a) ZT; (b) ZTN; (c) ZTC.

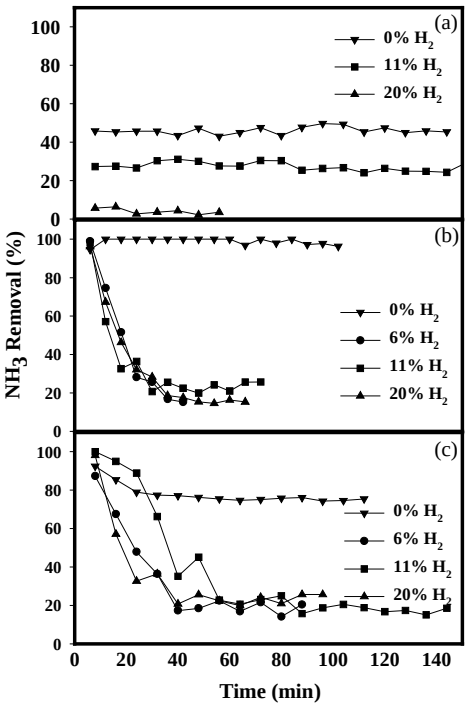

Fig. 7. NH_3 decomposition of various sulfurized sorbents with various H_2 concentrations: (a) ZT; (b) ZTN; (c) ZTC.

From these results, it was concluded that the cobalt oxide within ZTC sorbent was a better catalyst for the NH_3 decomposition reaction than the nickel oxide in the ZTN sorbent. Fig. 7 shows the NH_3 decomposition of various sorbents at different H_2 concentrations after sulfidation with H_2S. The NH_3 decomposition of ZT sorbent showed 0–40% with H_2 concentration which was similar to the results observed in the empty reactor. This result indicates that ZnS did not participate in NH_3 decomposition. NH_3 decomposition of ZTN and ZTC sorbents was 100% at the initial period and then rapidly dropped with reaction times in the presence of H_2, even though it showed 100 and 75% in the absence of H_2 and did not decrease with reaction times. Considering that most of the metal oxides were transformed to metal sulfides after sulfidation, it was thought that the NH_3 decomposition over metal sulfides was less than that over metal oxides. Metal sulfide was affected more severely by H_2 compared with metal oxides. The decrease in the NH_3 decomposition over ZTN and ZTC sorbents with reaction time, as shown in Fig. 3, could be explained by deactivation due to the formation of metal sulfides and the effect of hydrogen in the mixed gas.

3.4. Reduction of sorbent

Fig. 8 shows the effect of hydrogen on the NH_3 decomposition of ZTN and ZTC sorbents in the presence of H_2S. As expected, the total sulfur removal capacity of both sorbents did not change. The NH_3 decomposition of the ZTC sorbent was 100% at the initial period without H_2. However, as time proceeded, they decreased until 75% which was maintained for a long time, as shown in Fig. 7. This result indicates that cobalt oxides reacted with the H_2S and were gradually transformed to cobalt sulfides. In the case of the ZTN sorbent, 100% of the NH_3 was decomposed at initial period and did not change with reaction time. When 10% of the H_2 was introduced into the reactor, the NH_3 decomposition over ZTN sorbent suddenly dropped to 20%, while that of the ZTC sorbent increased to 100% and then dropped to 20%. In addition,

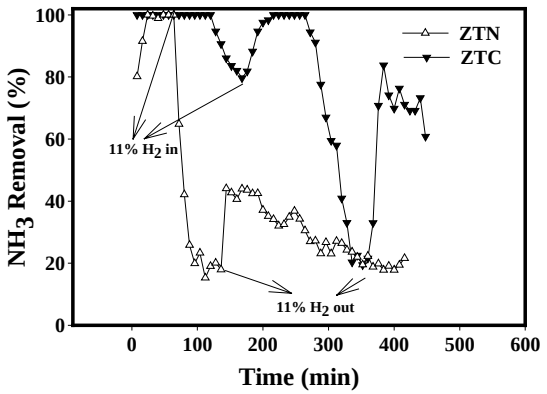

Fig. 8. The effect of hydrogen on the NH_3 decomposition of ZTN and ZTC sorbents.

when the addition of 10% of H_2 was stopped, it was also observed that NH_3 decomposition of the ZTC sorbent was recovered up to 75%, while that of the ZTN sorbent was not completely recovered. To explain the difference in the recovery of the NH_3 decomposition, the NH_3 decomposition on the ZTC and ZTN sorbents reduced with H_2 at 650 °C were investigated. NH_3 was decomposed completely in gas compositions without H_2 whether the sorbents were reduced or not. In the case of the sulfurized sorbent, as shown Fig. 9, ZTC sorbent showed higher reactivity than that of unreduced one, while ZTN sorbent showed 100% decomposition ability regardless of reduction state. Fig. 10 shows the NH_3 decomposition over reduced ZTC and ZTN sorbent in the presence of H_2S. NH_3 was decomposed completely on the reduced ZTC sorbent and the removal capacity was maintained until breakthrough point of 350 min. The increase in the removal capacity from 100 min of oxide sorbent to 350 min of reduced sorbent could be explained by the transformation of cobalt oxides with ZTC to a new reduced phase which could decompose NH_3 more effectively than unreduced oxides, even though the phase was not clearly defined. As shown in Fig. 8, it was concluded that the temporal increase of NH_3 decomposition on the ZTC sorbent when 11% hydrogen was injected is due to the phase transformation of the active sites, cobalt oxides and sulfides, to a new phase. In the case of ZTN sorbent, as shown in Fig. 10, NH_3 decomposition of reduced ZTN sorbent showed 60% removal capacity even at initial period and the value gradually decreased into 20% with reaction time. Considering that NH_3 decomposition of ZTN sorbent did not depend on the reduction states of the sorbent under gas compositions without H_2S as shown in Fig. 9, this result could be explained by the following reason: The oxygen within ZTN lattice would be consumed during reduction of sorbent and this reduced ZTN sorbent produces ZnS and H_2O through reaction between ZnO and H_2S under gas compositions with H_2S. At that time, if the oxygen within ZTN lattice is not enough, H_2O cannot be produced and H_2 decomposed from H_2S hinders NH_3 from decomposing to N_2 and H_2 due to equilibrium limitation. In addition, this phenomenon was not critical over ZTC sorbent, which can be explained that NH_3 decomposition of ZTC sorbent was less effective in the presence of H_2 than ZTN sorbent as shown in Fig. 6.

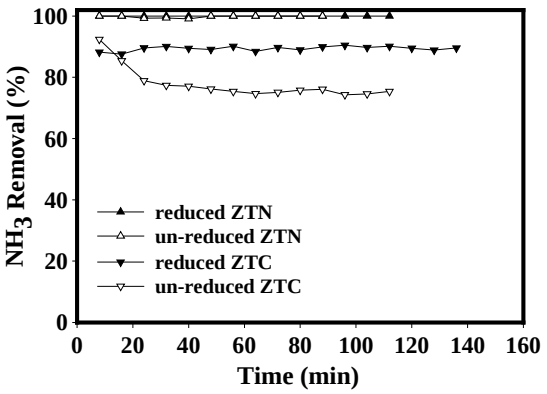

Fig. 9. NH_3 decomposition of the sulfurized ZTN and ZTC sorbent after various treatments in gas compositions without H_2 and H_2S.

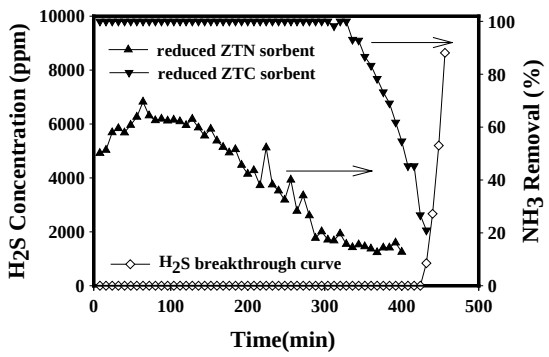

Fig. 10. H_2S breakthrough curve and NH_3 decomposition of reduced ZTC and ZTN sorbent at gas compositions without H_2.

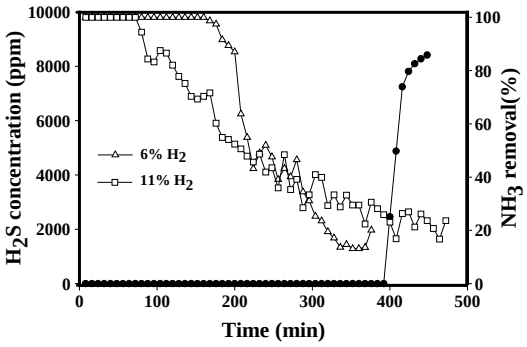

Fig. 11. Simultaneous removal of H_2S and NH_3 with H_2 concentrations.

3.5. Simultaneous removal of H_2S and NH_3

Fig. 11 shows the H_2S breakthrough curve and NH_3 decomposition of the ZTC sorbent various H_2 concentrations. The NH_3 decomposition decreased with increasing H_2 concentrations. As shown in the previous results, this could be explained by the fact that NH_3 decomposition was related with the phases (oxide or sulfides) of the sorbent, the reduction of sorbent, and the effect of product gases such as H_2. In the desulfurization process of the IGCC system using fluidized absorption and regeneration beds, if a half-spent sorbent was moved to the regeneration bed, the NH_3 decomposition was 100 and 60% in gas compositions with 6 and 10% H_2, respectively. As a result, we concluded that it was possible to simultaneously remove H_2S and NH_3 gases under strong reducing gas compositions of coal-derived gases.

4. Conclusions

NH_3 in fuel gases did not affect the sulfur removal capacity of Zn–Ti-based sorbents. The additives, cobalt and nickel, were found to be active components in the NH_3 decomposition as well as H_2S absorption, while major components such as ZnO and TiO_2 did not show any activity in the NH_3 decomposition reaction. NH_3 was decomposed over both oxide and sulfide forms of the additives, even though the NH_3 decomposition ability of their sulfides dramatically decreased in the presence of H_2 gas owing to the equilibrium limitations of NH_3 decomposition. In the case of oxide forms, cobalt oxide showed an excellent NH_3 decomposition capacity regardless of H_2 concentrations, while the capacity of nickel oxide depended on the H_2 concentrations.

Acknowledgements

We appreciate financial support from the R&D Management Center for Energy & Resources (RaCER, Korea) and also in part from Korea Ministry of Science and Technology through the National Research Lab. Program.

References

[1] K. Jothimurugesan, S.K. Gangwal, Ind. Eng. Chem. Res. 37 (1998) 1929.
[2] B.S. Turk, R.P. Gupta, US Patent 6,306,793 (2001).
[3] V. Rajagopalan, M.D. Amiridis, Ind. Eng. Chem. Res. 38 (1999) 3886.
[4] E. Sasaoka, N. Sada, A. Manabe, Md.A. Uddin, Y. Sakata, Ind. Eng. Chem. Res. 38 (1999) 958.
[5] R.V. Siriwardane, T. Gardner, J.A. Poston Jr., E.P. Fisher, A. Miltz, Ind. Eng. Chem. Res. 39 (2000) 1106.
[6] E.M. van Veldhuizen, L.M. Zhou, W.R. Rutgers, Plasma Chem. Plasma Process. 18 (1998) 91.
[7] E. Sasaoka, M. Hatori, N. Sada, Md.A. Uddin, Ind. Eng. Chem. Res. 39 (2000) 3844.
[8] H.K. Jun, T.J. Lee, S.O. Ryu, J.C. Kim, Ind. Eng. Chem. Res. 40 (2001) 3547.
[9] L. Alonso, J.M. Palacios, R. Moliner, Energy Fuels 15 (2001) 1396.
[10] L. Alonso, J.M. Palacios, Chem. Mater. 14 (2002) 225.
[11] M. Hatori, E. Sasaoka, Md.A. Uddin, Ind. Eng. Chem. Res. 40 (2001) 1884.
[12] H.K. Jun, T.J. Lee, J.C. Kim, Ind. Eng. Chem. Res. 41 (2002) 4733.
[13] J.V. Ibarra, C. Cilleruelo, E. Garcia, M. Pineda, J.M. Palacios, Vib. Spectrosc. 16 (1998) 1.
[14] R.B. Slimane, J. Abbasian, Ind. Eng. Chem. Res. 39 (2000) 1338.
[15] T. Hasegawa, M. Sato, Combust. Flame 114 (1998) 246.
[16] S.K. Gangwal, R.P. Gupta, J.W. Portzer, B.S. Turk, K. Jothimurugesan, in: Proceedings of the Conference on Advanced Coal based Power and Environmental System'97, DOE/FTC-97/1046, 1997.
[17] G.B. Kim, Y.S. Park, C.K. Ryu, S.H. Cho, G.T. Jin, C.K. Yi, Theories Appl. Chem. Eng. 5 (1999) 3549.
[18] R.P. Gupta, B.S. Turk, T.C. Merkel, G.N. Krishnan, D.C. Ciero, in: Proceedings of the Conference on 17th Annual Pittsburgh Coal, September 2000.

[19] S.A. Qader, Q.A. Qader, L.J. Muzio, in: Proceedings of the Advanced Coal-fired Power Systems'96 Review Meeting, July 16–17, 1996.
[20] W. Mojtahed, J. Abbasian, Fuel 74 (1995) 1698.
[21] Z.R. Ismagilov, R.A. Shkrabina, S.A. Yashnik, N.V. Shikina, I.P. Andrievskaya, S.R. Khairulin, V.A. Ushakov, J.A. Moulijin, I.V. Babich, Catal. Today 69 (2001) 351.
[22] S.K. Gangwal, R.P. Gupta, J.W. Portzer, B.S. Turk, G.N. Krishnan, S.L. Hung, R.E. Ayala, in: Proceedings of the Advanced Coal-fired Power Systems'96 Review Meeting, July 16–17, 1996.
[23] R.E. Ayala, C. Park, US Patent 5,188,811 (1993).
[24] J. Hepora, P. Simell, Appl. Catal. B 14 (1997) 305.
[25] W. Wong, N. Padban, Z. Ye, A. Andersson, I. Bjerle, Ind. Eng. Chem. Res. 38 (1999) 4175.